Dalton Transactions

Accepted Manuscript

ROYAL SOCIETY OF CHEMISTRY

www.rsc.org/dalton

Journal Name

ARTICLE

The Flexibility of Modified-Linker MIL-53 Materials

Alexis S. Munn,[a] Renjith S Pillai,[b] Shyam Biswas,†[c] Norbert Stock[c], Guillaume Maurin*[b] and Richard I. Walton*[a]

Received 00th January 20xx,
Accepted 00th January 20xx

DOI: 10.1039/x0xx00000x

www.rsc.org/

The flexibility of eight aluminum hydroxo terephthalates [Al(OH)(BDC-X)]·n(guest) (BDC = 1,4-benzene-dicarboxylate; X = -H, -CH_3, -Cl, -Br, -NH_2, -NO_2, -$(OH)_2$, -CO_2H) crystallising in the MIL-53-type structure was investigated upon thermal dehydration of as-made samples, superhydration and methanol adsorption/desorption using *in situ* powder X-ray diffraction (PXRD). Profile fitting was used to determine lattice parameters as a function of time and/or temperature to describe their structural evolution. It has thus been shown that while methanol vapour adsorption induces an opening of all the modified frameworks, except the -NH_2 material, superhydration only leads to open structures for Al-MIL-53–NO_2, –Br and –$(OH)_2$. All the MIL-53 solids, except Al-MIL-53–$(OH)_2$ are present in the open structures upon thermal dehydration. In addition to the exploration of the breathing behavior of this MIL-53 series, the issue of disorder in the distribution of the functional groups between the organic linkers was explored. As a typical illustration, density functional theory calculations were carried out on different structures of Al-MIL-53-Cl, in which the distribution of –Cl within two adjacent BDC linkers is varied. The results show that the most energetically stable configuration leads to the best agreement with the experimental PXRD pattern. This observation supports that the distribution of the selected linker substituent in the functionalised solid is governed by energetics and that there is a preference for an ordering of this arrangement.

Introduction

Metal-organic frameworks (MOFs) are hybrid porous materials that have been widely studied due to their promise in several fields of application.[1] One distinctive property of MOFs, compared to traditional zeotype porous materials, is their structural flexibility, which may be due to the connection of organic ligands with inorganic building units, and this can give rise to conformational variability.[2] Among the large number of reported MOFs, only a few exhibit a fully reversible transition between different framework conformations that is triggered by an external stimulus, such as temperature, pressure or the presence of guest molecules.[3] A particularly interesting set of MOFs that shows a spectacular phenomenon known as 'breathing' is the MIL-53 series (MIL stands for Materials of Institute Lavoisier).[4,5,6,7,8] The structure of MIL-53 is built up by the interconnection of infinite chains of *trans* corner-sharing MO_6 polyhedra (where M designates a trivalent metal cation) and linear dicarboxylate ions that leads to a 3D solid with lozenge-shaped channels.[5,8] The breathing phenomenon associated with this family of solids corresponds to a stimulus induced structural transition between an open and a closed phase involving a significant volume change up to 40 %.[9] Until now several metal ions were found to form this framework structure, including Sc^{3+}, V^{3+}, Cr^{3+}, Fe^{3+}, Al^{3+}, Ga^{3+} and In^{3+}.[5,8,10] The structural behaviours of this family of solids have been studied under a wide variety of conditions and the use of functionalised organic linkers has been shown to have a profound impact on the breathing and hence on their properties of interest for diverse areas such as gas adsorption/separation and proton conduction.[11,12,13,14,15,16]

Herein we describe the structural behaviour of eight functionalized Al-MIL-53 materials (BDC-X with X -H, -CH_3, -Cl, -Br, -NH_2, -NO_2, -$(OH)_2$, -CO_2H) under different experimental conditions (thermal dehydration, superhydration, methanol adsorption/desorption) using powder X-ray diffraction (PXRD). This method allows the determination of the unit cell parameters of the material under these different conditions, but does not allow the crystal structure of these solids to be deduced due to a combination of the inherent low resolution of the laboratory PXRD technique and the possibility of disorder in the position of the modifying groups on the linkers. In order to shed light into the question of location of ligand substituents, which may be of relevance to other families of functionalised MOF materials, density functional theory (DFT) calculations were performed on different configurations that

[a] *Department of Chemistry, University of Warwick, Coventry, CV4 7AL, United Kingdom.*
[b] *Institut Charles Gerhardt Montpellier, UMR CNRS 5253, Université Montpellier, 34095 Montpellier cedex 05, France.*
[c] *Institut für Anorganische Chemie, Christian-Albrechts-Universität, Max-Eyth Straße 2, D 24118 Kiel, Germany.*
†Present address: Department of Chemistry, Indian Institute of Technology Guwahati, 781039 Assam, India
Corresponding authors: Guillaume Maurin, guillaume.maurin@univ-montp2.fr, Richard I. Walton, R.I.Walton@warwick.ac.uk; Electronic Supplementary Information (ESI) available: [details of any supplementary information available should be included here]. See DOI: 10.1039/x0xx00000x

differ by the distribution of their grafted functions with a focus on the Cl-version of this solid.

Experimental

Materials

The functionalised Al-MIL-53 samples were synthesised and characterised according to previously published procedures.[17]

In situ Powder X-ray Diffraction (PXRD)

A Bruker D8 diffractometer operating with Cu $K\alpha_{1/2}$ radiation was used for these experiments, as described in previous work on Fe-MIL-53.[18] The sample packed into a Macor holder and data measured in θ–θ geometry using a VÅNTEC solid-state detector, which permitted a typical diffraction pattern to be accumulated in around 3 min. The diffractometer was equipped with an Anton Parr XRK 900 reactor chamber which allowed gases to be passed over the sample and also permitted controlled heating to observe thermal evolution of samples. Either dry nitrogen was used, or the nitrogen was bubbled through methanol in a Drechsel bottle to introduce a vapour of solvent over the sample. The powdered sample was packed into the holder to allow space for expansion and its height was checked after the experiment to ensure that no movement had occurred. 'Superhydration' experiments were also performed and in this case the powdered MOF was mixed with a few drops of water to form a paste and powder diffraction measured immediately. Profile analysis (Le Bail intensity fitting with refinement of lattice parameters) of individual powder X-ray patterns was performed using the GSAS suite of software,[19] implemented within EXPGUI.[20]

Density Functional Theory Calculations

Four plausible structures of Al-MIL-53-Cl which differ by the distribution of –Cl within two adjacent BDC linkers, i.e. BDC connecting the –Al–OH–Al chains were generated by a ligand replacement strategy starting with the non-functionalised Al-MIL-53 structure (Figure 1). These structure models were geometry optimized in *P*1 symmetry by DFT calculations allowing the relaxation of the atomic positions while maintaining the unit cell parameters to those experimentally determined (a = 16.716 Å, b = 12.899 Å, c = 6.6376 Å, V = 1431.3 Å^3). These calculations were performed using the PBE[21] functional along with a combined Gaussian basis set and pseudopotential in the CP2K package.[22-25] In the case of carbon, oxygen, chlorine and hydrogen, a triple zeta (TZVP-MOLOPT)[26] basis set was considered while a double zeta (DZVP-MOLOPT)[26] was applied for Al. The pseudopotentials used for all the atoms were those derived by Goedecker, Teter and Hutter.[27] The van der Waals interactions were taken into account via the use of semi-empirical dispersion corrections as implemented in the DFT-D3 method.[28]

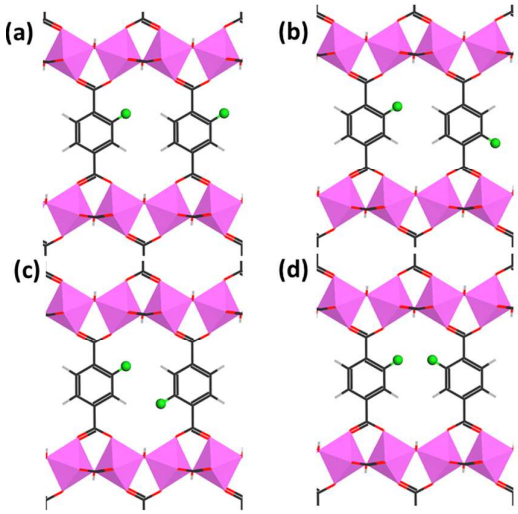

Figure 1: Schematic representation of the plausible distributions of –Cl in Al-MIL-53-Cl labelled as (a) A, (b) B, (c) C and (d) D (colour code: Al, pink; C, gray; O, red; Cl, green; H, white.

Results and discussion

Structural flexibility

Taking the Al-MIL-53-Cl as an example, Figure 2a shows the thermal evolution of the material. The hydrated, phase of the –Cl modified Al-MIL-53 framework has a C-centred monoclinic unit cell volume of 993 Å^3 with the profile fit performed in the *C*2/*c* spacegroup. The thermal dehydration experiment shows that the framework expands to a fully-open phase when heated above 190 °C. Subsequent cooling back to 30 °C shows that the framework remains open until 110 °C and then even at room temperature an amount of the open phase remains (Supporting Information). Figure 2b shows the Le Bail profile fit for the dehydrated, open phase; a longer data collection was used while the sample was held at 210 °C to achieve the statistics necessary for this fit. This analysis confirms that the dehydrated material has the orthorhombic, *Imcm,* structure with a unit cell volume of 1431.3 Å^3.

The superhydration experiment showed that the –Cl modified framework only partially expands in the presence of excess water; the majority of the framework remains closed. A two-phase Le Bail profile fit was performed, using the data collected *in situ*, and the result is shown in Figure 3. The refinement confirms that the majority of the sample remains unchanged with the *C2/c* structure and only a small amount of the sample expands to the *Imcm* structure.

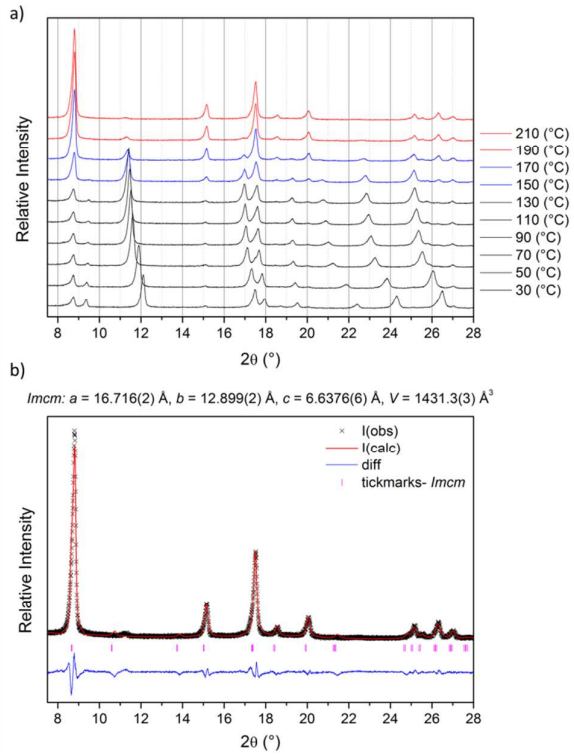

Figure 2: Thermal dehydration of –Cl modified Al-MIL-53. a) Individual XRD patterns showing a change in structure with increasing temperature (Black = hydrated phase (*C*2/*c*), blue = mixed phase and red = dehydrated phase(*Imcm*)) and b) Le Bail profile fit for data recorded at 210 °C.

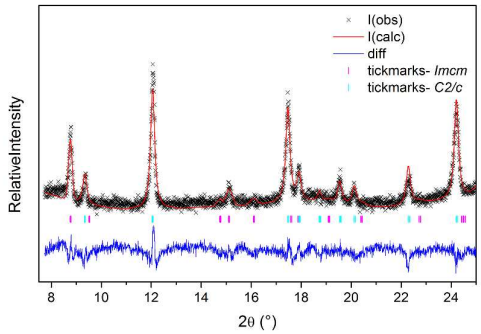

Figure 3: Le Bail profile fit for the superhydrated –Cl modified Al-MIL-53. The *Imcm* space group was used to model the fully-open structure (pink tick marks) and the space group *C*2/*c* was used to model the closed structure (pale blue tick marks).

Figure 4a shows the behaviour of the -Cl modified framework in response to methanol vapour that was added at scan 4 (point A on Figure 4a). The hydrated phase shows some gradual expansion, where the transient peaks at around scans 10-20 represent a partially open phase that probably contains a mixture of water and methanol as was seen for Fe-MIL-53 previously,[18] before expanding completely to the fully-open phase. The methanol vapour was replaced by a pure flow of nitrogen gas on scan 85 (point B), it can be seen that the flow of nitrogen was not sufficient to remove the methanol from the pores even after more than four hours. A Le Bail profile fit was performed on an individual pattern from the *in situ* data (Figure 4b). Although this pattern has a low signal-to-noise ratio it was possible to obtain unit cell parameters that confirm that the sample has the fully-open *Imcm* structure upon addition of methanol vapour. This refinement gave a unit cell volume of 1411 Å^3, which is slightly smaller than its corresponding dehydrated phase (1431 Å^3) despite the fact that no strong interactions are expected between the additional –Cl groups and the MeOH guest molecules that might result in a contraction of the framework.

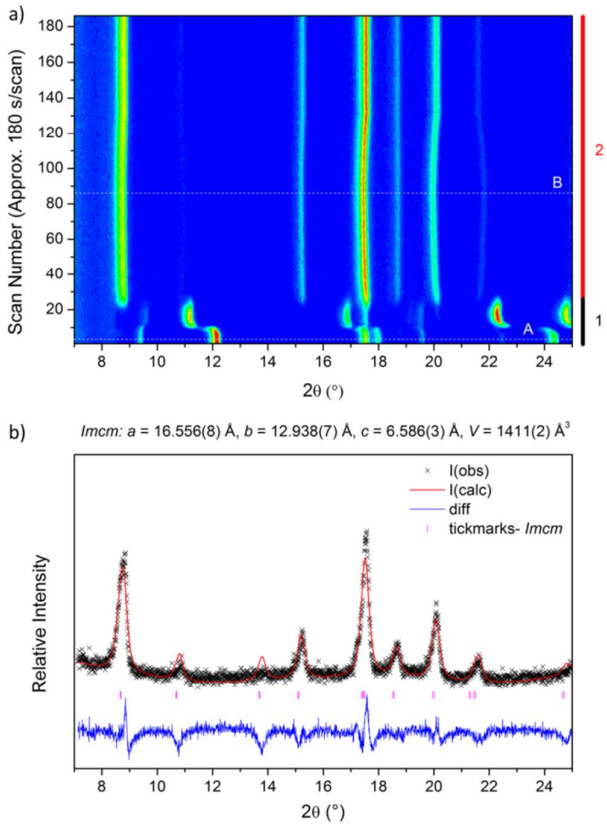

Figure 4: Behaviour of the –Cl modified Al-MIL-53 towards methanol vapour. a) Contour plot showing the change in symmetry of the framework as methanol is taken up (Phase 1 (black) = hydrated phase(s) (*C*2/*c*) and Phase 2 (red) = fully-open phase (*Imcm*)) and b) Le Bail profile fit for the fully-open phase

Journal Name

ARTICLE

Table 1: Cell volumes of various modified Al-MIL-53 frameworks compared with the unmodified framework as determined by *in situ* powder XRD. More detailed information including the unit cell parameters are listed in the supporting information. SG = spacegroup.

	Hydrated		Dehydrated		Superhydrated		Methanol	
	V / Å^3	Symmetry	V / Å^3	SG	V / Å^3	SG	V / Å^3	SG
-H	946.8[a]	*Cc*	1412.0	*Imma*[a] *170 °C*	not studied		not studied	
-NO_2	1032.1(1)[b]	*C*-monclinic	1420.9(4)	*Imma 210 °C*	1511.5(4)	*Imcm* (major)	1467.6(3)	*Imcm*
					1082.0(4)	*C2/c*		
-Br	1055.1(2)[b]	*C*-monclinic	1420.6(1)	*Imcm 210 °C*	1471(1)	*Imcm*	1476.7(1)	*Imcm*
-CH_3	998.1(2)[b]	*C*-monclinic	1416.6(2)	*Imcm 190 °C*	1438.4(4)	*Imcm* (major)	1450.2(1)	*Imcm*
					1020.1(4)	*C2/c*		
-$(OH)_2$	954.9(5)[b]	*C*-monclinic	903.6(2)	*C2/c*	1397.6(5)	*Imcm*	1444.5(2)	*Imcm*
-COOH	1054.7(4)[c]	*Cc*	1434.2(2)	*Imcm 310 °C*	1460.0(6)	*Imcm* (major)	1440(1)	*Imcm*
					1059.6(9)	*C2/c*		
-Cl	993.0(5)[b]	*C*-monclinic	1431.3(3)	*Imcm 190 °C*	1499(1)	*Imcm*	1411(2)	*Imcm*
					994.4(3)	*C2/c* (major)		
-NH_2	961.5(10)[b]	*C*-monclinic	no change		no change		no change	

a: data taken from reference 5, b: data taken from reference 17, c: data taken from reference 13.

The other seven materials were studied in the same way and Table 1 summarizes the results of the powder diffraction experiments (all plots of data are provided in Supporting Information). For comparison the results from the unmodified material are also included, *i.e.* Al-MIL-53.[5] It is clear that the modified Al-MIL-53 materials show differing flexibility depending on the nature of the substituent on the linker. The amino-modified framework shows no flexibility under all conditions studied. This observation is consistent with what has been previously reported by Stavitski *et al.*[29] for the same solid upon CO_2 adsorption, and also Lescouet *et al.* who found no pore opening upon heating.[30] This may be attributed to a relatively strong hydrogen bonding interactions between the NH_2 group and the μ_2-OH groups of the AlO_6 polyhedra that stabilises the closed form with respect to the open form thus preventing the reopening of the structure whatever the external stimuli.

The dehydration experiments using thermal treatment showed that all of the other frameworks, except the –$(OH)_2$ modified form, present fully-open structures with very similar unit cell volumes ranging from 1412.0 Å^3 (-H form) to 1434.2(2) Å^3 (–CO_2H). The small unit cell differences can be attributed to the size and the number of functional groups.

The –NO_2 modified framework is dehydrated most easily, showing complete conversion to the fully open form at 170 °C. The –CO_2H modified framework is the most difficult to dehydrate, where complete conversion to the fully-open phase is not seen until 310 °C. This is consistent with relatively strong interactions between H_2O and this acidic function as evidenced in other –CO_2H functionalized MOFs.[31] In contrast to the other frameworks, the –$(OH)_2$ modified framework contracts during thermal treatment and this contraction is complete by 110 °C. Furthermore, all of the frameworks showed some hysteresis upon cooling to room temperature; the frameworks remained in their respective dehydrated phases to temperatures lower than those required to dehydrate them. While this might be explained by a higher stability of the closed form vs open form resulting from the hydrogen bonding interactions between the 2 –OH grafted functions and the μ_2-OH groups present at the MOF surface, it should be borne in mind that the kinetics of aerial rehydration are likely to be slow in the sample chamber.

The superhydration experiments showed that only three of the modified frameworks, –NO_2, –Br and –$(OH)_2$, could be fully

superhydrated under such experimental conditions to give the open structure. Previously the Cr version of MIL-53 was shown to have similar behaviour in excess water.[32] The $–CH_3$ and $–CO_2H$ modified frameworks give a majority of the sample superhydrated, whereas only a small amount of the –Cl modified sample was superhydrated using the same experimental conditions. This observation suggests that the interaction of water strongly depends on the nature of the ligand's functional groups, being weaker for the $–CH_3$, $–CO_2H$ and –Cl functionalised materials. It was further found that the excess water molecules can be easily removed at 30°C with a flow of N_2 gas for most of the materials studied. The exception is the $–NO_2$ modified framework that requires heat to remove the excess water from the pores, indicating that this material shows the strongest interaction with water. As reviewed by Canivet *et al.*, the decoration of ligands with functional groups can adjust the adsorption isotherms of MOFs towards water in isostructural families,[33] and the total uptake of water can be tuned by the nature of the functional group. Our *in situ* powder X-ray diffraction data provide a complementary way to examine this phenomenon.

The methanol vapour adsorption experiments show that all of the modified frameworks could be opened fully in the presence of methanol vapour, as seen previously for Fe-MIL-53.[18] The refined unit cells show that the fully-open methanol phases are, in general, larger than the fully-open dehydrated phases. Desorption of methanol was achieved by passing pure N_2 gas over the sample to remove the methanol from the pores. The $–NO_2$ and $–CH_3$ modified frameworks show a slight contraction upon the introduction of the N_2 gas which is consistent with a contraction to the slightly smaller pore volume of the fully-open dehydrated phase. The –Cl modified framework shows very little change, while the $–(OH)_2$ and $–CO_2H$ modified frameworks both exhibit a change in framework symmetry upon the introduction of N_2 gas; they both contract to a pore volume similar to the half-open phase seen for Fe-MIL-53.[18] Fe-MIL-53 was shown to contain two equivalents of methanol when the framework was fully-open and one equivalent of methanol when the framework was half-open.[18] The half-open phase seen for these two frameworks could be the result of the methanol guest being lost in two stages. This would suggest that the removal of both equivalents of methanol from these frameworks was not possible using just a flow of N_2 gas.

The conclusion of these experiments is that the breathing behaviour of ligand-modified Al-MIL-53 and its kinetics are dependent on the chemical nature of the functional groups. This is likely to be triggered by an interplay between the intra-framework interactions, *e.g.* hydrogen bonding between the grafted functions and the μ_2-OH groups, and the strength of interactions between these functions and the guest molecules. Functionalisation of the linker molecules thus provides a method of tuning the flexibility of the structure, of relevance to separation or sensing applications.

Disorder in Al-MIL-53-Cl

Figure 5 reports the DFT optimized crystal structures for the 4 different Al-MIL-53-Cl models, labeled as A, B, C and D. The total electronic energy for each DFT-optimized configuration is provided in Table 2. The energy sequence follows the trend: A<B <C <D. Models C and D are the less stable structures since they correspond to the cases where the Cl atoms of two adjacent ligands are in very close vicinity (with Cl-Cl characteristic distances of 3.6-3.8 Å) leading to a relatively strong Cl/Cl repulsion interaction which contributes to destabilise the structure. In contrast, the Cl atoms are separated by much longer distances in A and B while Table 2 reveals that the halogen in these situations can establish relatively strong interactions with the μ_2-OH groups (Cl- μ_2-OH characteristic distances of 2.7-2.8 Å), as was already evidenced in the Fe-MIL-53-Cl solid, and this also contributes to the stability of these two structures.[34] Further, while the non-functionalised Al-MIL-53 solid shows a distribution of Al–Oc–Cc–Cg dihedral angle at 180° with a perfect planarity of the phenyl ring,[7] Figure 6 reveals that, for the Al-MIL-53-Cl, the corresponding angle values are 170° - 180° or 160°-180° for A and B respectively. Indeed, configuration B is characterised by a slightly more pronounced geometric constraint associated with a tilting of the organic linker and this causes the lower stability of B compared to A.

Al-MIL-53-Cl	Energy /kJ mol^{-1}	ΔE /kJ mol^{-1} [a]
A	-3052849.7569	0.0000
B	-3052846.6401	3.1168
C	-3052836.3170	13.4398
D	-3052833.2054	16.5514

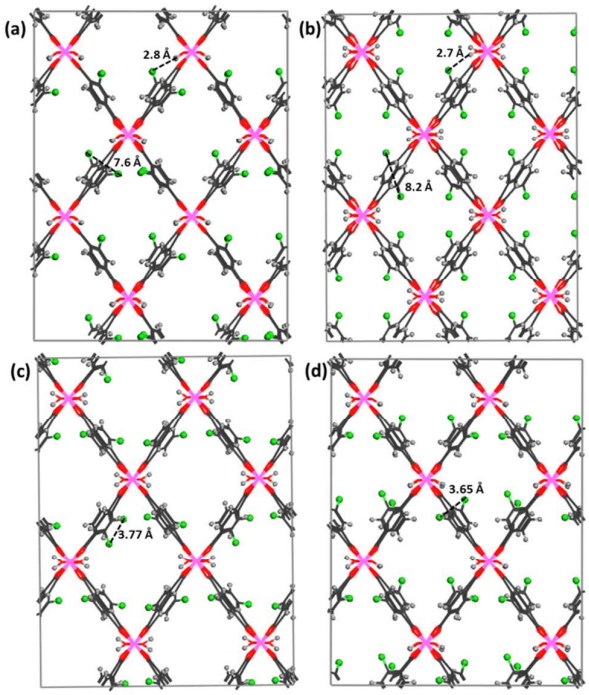

Figure 5: DFT-geometry optimized structures of the four different Al-MIL-53-Cl A (a), B (b), C (c), and D (d) viewed along the c axis (colour code is same as in Figure 1).

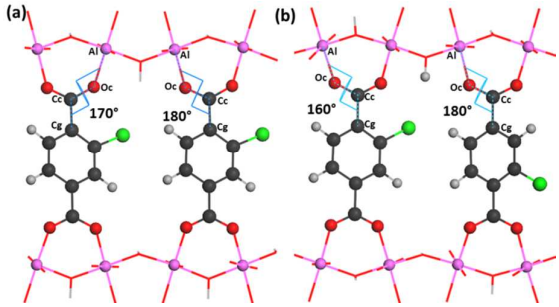

Figure 6: Illustration of the Al–Oc–Cc–Cg dihedral angle observed from DFT-geometry optimized structures of the two different A (a) and B (b) configurations (colour code is same as in Figure 1).

These calculations clearly emphasise that the plausible configurations generated by a various distributions of the functionalised groups show distinct energies although we cannot exclude that some of them can co-exist, i.e. A and B, since their energy differences are only slightly higher than the thermal energy at room temperature (3.1 kJ.mol^{-1} vs 2.3 kJ.mol^{-1}, see Table 2).

Table 2: Total electronic energy and some selected structural features for all the optimised Al-MIL-53-Cl configurations
[a] Relative energy ranking

As a validation step of these theoretical findings, the PXRD patterns for each configuration were calculated and compared to the experimental data collected on the Al-MIL-53-Cl sample. Figure 7 shows that the most energetically stable configuration A leads to the best agreement with the experimental PXRD pattern. This observation suggests that the distribution of the grafted functions in the functionalized Al-MIL-53-Cl solid is governed by energetics and that there is an ordering of this arrangement. The presence of a small amount for configuration B, however, cannot be ruled out, and this disorder may explain the peak broadening seen in the patterns.

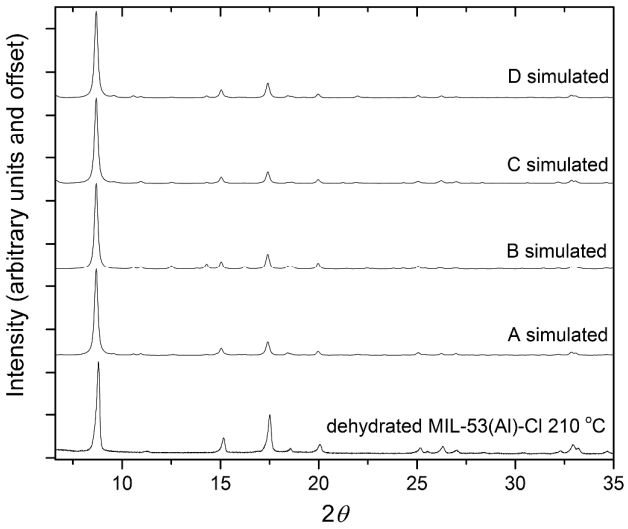

Figure 7: Experimental and simulated XRD pattern for optimized Al-MIL-53-Cl with plausible Cl distribution at its linker: configurations A, B, C and D (Cu Kα1/2 radiation).

Conclusions

Our study provides new results that show how the flexibility of linker-modified forms of MIL-53 is strongly influenced by the chemical nature of the linker. PXRD analysis shows that all the functionalised Al-MIL-53 solids studied, except the amino-modified form, exhibit a breathing behaviour upon thermal treatment and liquid, vapour adsorption/desorption that can be tuned by changing the nature of the grafted functions. This structural breathing is controlled by both the host/guest and intra-framework interactions, and for some materials particularly strong host-guest interactions are clearly evidenced, for example in the case of the nitro-modified material where once water is introduced it is subsequently very difficult to remove, leaving the solid in a superhydrated state. Methanol is adsorbed effectively and reversibly by all

solids, except the amino material, which may be due to the volatility of the liquid guest, even when bulky substituents such as bromo- or nitro- are present. Using the chloro-modified material as a case study, DFT calculations reveal that the distribution of the ligand-grafted functions is most probably ordered in the crystal structure due to a combination of steric effects and favourable interactions with framework μ_2-OH groups, but minor contributions of other energetically similar configurations cannot be ruled out, and this disorder may explain the relatively broadened powder XRD profiles seen for the materials.

Acknowledgements

The research leading to these results has received funding from the European Community's Seventh Framework Programme (FP7/2007-2013) under Grant Agreement No. 228862. G.M. acknowledges Institut Universitaire de France and N.S. the DFG (SPP-1362) for support. The equipment used in materials characterisation at the University of Warwick was obtained through the Science City Advanced Materials project "Creating and Characterising Next Generation Advanced Materials" with support from Advantage West Midlands (AWM) and part funded by the European Regional Development Fund (ERDF).

Notes and references

1 a) Themed issue *Chem. Rev.* 2012, **112**, 673; b) Themed issue *Chem. Soc. Rev*. 2014, **43**, 5415; c) D. Farrusseng (Ed) Metal-Organic Frameworks: Applications from Catalysis to Gas Storage, Wiley-VCH Verlag & Co KgaA, Weinheim, (2011); d) L.R. MacGillivray and C.M. Lukehart (Eds) Metal-Organic Framework Materials. John Wiley & Sons Ltd , Chichester (2014).

2 a) K. Uemura, R. Matsuda and S. Kitagawa, *J. Solid State Chem.* 2005, **178**, 2420; b) G. Férey and C. Serre, *Chem. Soc. Rev.* 2009, **38**, 1380.

3 A. Schneeman, V. Bon, I. Schwedler, I. Senkovska, S. Kaskel and R.A. Fischer, *Chem. Soc. Rev.* 2014, **43**, 6062.

4 G. Férey, *Chem. Soc. Rev.* 2008, **37**, 191.

5 T. Loiseau, C. Serre, C. Huguenard, G. Fink, F. Taulelle, M. Henry, T. Bataille and G. Ferey, *Chem.- Eur. J.,* 2004, **10**, 1373.

6 F. Niekiel, J. Lannoeye, H. Reinsch, A.S. Munn, A. Heerwig, I. Zizak, S. Kaskel, R.I. Walton, D. de Vos, P. Llewellyn, A. Lieb, G. Maurin and N. Stock, *Inorg. Chem.* 2014, **53**, 4610.

7 P. G. Yot, Z. Boudene, J. Macia, D. Granier, L. Vanduyfhuys, T. Verstraelen, V. Van Speybroeck, T. Devic C. Serre, G. Férey, N. Stock and G. Maurin, *Chem. Comm.* 2014, **50**, 9462.

8 C. Serre, F. Millange, C. Thouvenot, M. Noguès, G. Marsolier, D. Louër and G. Férey, *J. Am. Chem. Soc.* 2002, **124**, 13519.

9 G. Férey, C. Serre, T. Devic, G. Maurin, H. Jobic, P.L. Llewellyn, G. de Weireld, A. Vimont, M. Daturi and J.S. Chang, *Chem. Soc. Rev*. 2011, **40**, 550.

10 a) J. P. S. Mowat, S. R. Miller, A. M. Z. Slawin, V. R. Seymour, S. E. Ashbrook and P. A. Wright, *Micropor. Mesopor. Mat.* 2011, **142**, 322; b) K. Barthelet, J. Marrot, D. Riou and G. Ferey, *Angew. Chem. Int. Edt.* 2002, **114**, 291; c) T. R. Whitfield, X. Wang, L. Liu and A. J. Jacobson, *Solid Stat. Sci.* 2005, **7**, 1096; d) C. Volkringer, T. Loiseau, N. Guillou, G. Ferey, E. Elkaim and A. Vimont, *Dalton Trans*. 2009, 2241; e) V. Anokhina, M. Vougo-Zanda, X. Wang and A. J. Jacobson, *J. Am. Chem. Soc.* 2005, **127**, 15000.

11 T. Devic, P. Horcajada, C. Serre, F. Salles, G. Maurin, B. Moulin, D. Heurtaux, G. Clet, A. Vimont, J. M. Greneche, B. Le Ouay, F. Moreau, E. Magnier, Y. Filinchuk, J. Marrot, J. C. Lavalley, M. Daturi and G. Férey, *J. Am. Chem. Soc.*, 2010, **132**, 1127.

12 P. A. P. Mendes, P. Horcajada, S. Rives, H. Ren, A. E. Rodrigues, T. Devic, E. Magnier, P. Trens, H. Jobic, J. Ollivier, G. Maurin, C. Serre and J. A. C. Silva, *Adv. Funct. Mater.*, 2014, **24**, 7666.

13 N. Reimer, B. Gil, B. Marszalek and N. Stock, *CrystEngComm*, 2012, **14**, 4119.

14 A. Shigematsu, T. Yamada and H. Kitagawa, *J. Am. Chem. Soc.*, 2011, **133**, 2034.

15 S. Couck, E. Gobechiya, C.E.A. Kirschhock, P. Serra-Crespo, J. Juan-Alcaniz, A. Martinez Joaristi, E. Stavitski, J. Gascon, F. Kapteijn, G.V. Baron and J.F.M. Denayer, *Chem. Sus. Chem.* 2012, **5**, 740.

16 T. Devic, F. Salles, S. Bourrelly, B. Moulin, G. Maurin, P. Horcajada, C. Serre, A. Vimont, J.-C. Lavalley, H. Leclerc, G. Clet, M. Daturi, P.L. Llewellyn, Y. Filinchuke and G. Férey, *J. Mater. Chem.* 2012, **22**, 10266.

17 S. Biswas, T. Ahnfeldt and N. Stock, *Inorg. Chem.* 2011, **50**, 9518.

18 A.S. Munn, A.J. Ramirez-Cuesta, F. Millange and R.I. Walton, *Chem. Phys.* 2013, **427**, 30.

19 A.C. Larson and R.B. Von Dreele, in: Los Alamos National Laboratory Report LAUR, 1994, 86.

20 B.H. Toby, *J. Appl. Cryst.* 2001, **34**, 210.

21 J. P. Perdew, *Phys Rev B*, 1986, **33**, 8822.

22 J. VandeVondele, M. Krack, F. Mohamed, M. Parrinello, T. Chassaing and J. Hutter, *Comput Phys Commun*, 2005, **167**, 103.

23 J. VandeVondele and J. Hutter, *J. Chem. Phys.*, 2003, **118**, 4365.

24 G. Lippert, J. Hutter and M. Parrinello, *Theor Chem Acc*, 1999, **103**, 124.

25 G. Lippert, J. Hutter and M. Parrinello, *Mol. Phys.*, 1997, **92**, 477.

[26] J. VandeVondele and J. Hutter, *J Chem. Phys.*, 2007, **127**, 114105.
[27] S. Goedecker, M. Teter and J. Hutter, *Phys. Rev. B*, 1996, **54**, 1703.
[28] S. Grimme, J. Antony, S. Ehrlich and H. Krieg, *J Chem. Phys.*, 2010, **132**, 154104.
[29] E. Stavitski, E. A. Pidko, S. Couck, T. Remy, E. J. M. Hensen, B. M. Weckhuysen, J.Denayer, J. Gascon and F. Kapteijn, *Langmuir,* 2011, **27,** 3970.
[30] T. Lescouet , E. Kockrick , G. Bergeret , M. Pera-Titus and D. Farrusseng, *Dalton Trans.,* 2011, **40**, 11359.
[31] F. Ragon, B. Campo, Q. Yang, C. Martineau, A. D. Wiersum, A. Lago, V. Guillerm, C. Hemsley, J.F. Eubank, M. Vishnuvarthan, F. Taulelle, P. Horcajada, A. Vimont, P.L. Llewellyn, M. Daturi, S. Devautour-Vinot, G. Maurin, C. Serre, T. Devic and G. Clet, *J. Mater. Chem. A*, 2015, **3**, 3294.
[32] N. Guillou, F. Millange and R.I. Walton, *Chem. Commun.* 2011, **47**, 713.
[33] J. Canivet, A. Fateeva, Y. Guo, B. Coasne and D. Farrusseng, *Chem. Soc. Rev.*, 2014,**43**, 5594.
[34] B. Moulin, F. Salles, S. Bourrelly, P. L. Llewellyn, T. Devic, P. Horcajada, C. Serre, G. Clet, J. C. Lavalley, M. Daturi, G. Maurin and A. Vimont, *Micropor Mesopor Mat*, 2014, **195**, 197.

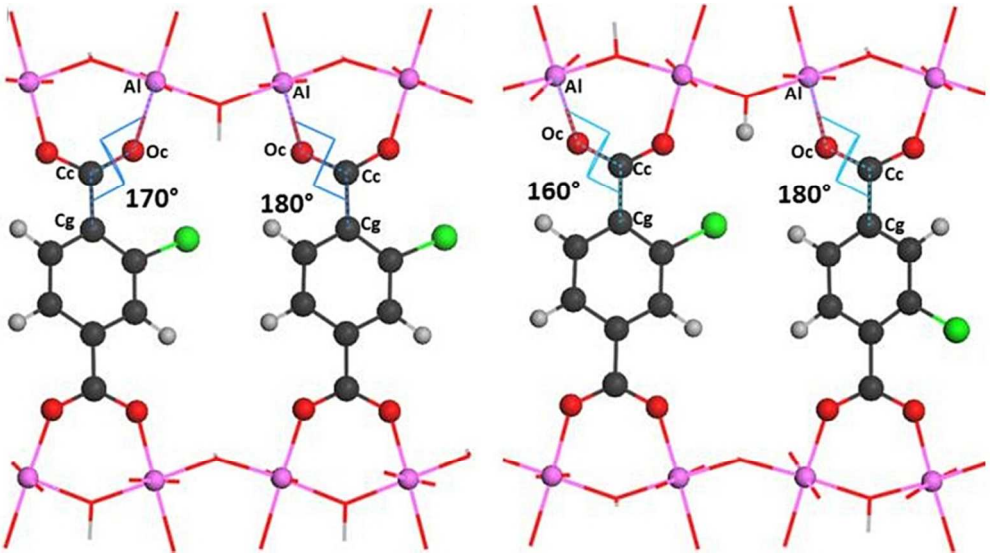

82x45mm (300 x 300 DPI)